

***In Silico* Drug Design and Molecular Docking Study of Some Related Structural Isomers of Nocodazole Analogues as Tubulin-Polymerization Inhibitors**

Suchaya Pongsai

Department of Chemistry, Faculty of Science, Burapha University, Chonburi
20131, THAILAND

Corresponding author. E-mail: busakorn@go.buu.ac.th

ABSTRACT

The molecular docking simulation and ADMET prediction have been performed to calculate and predict the new available drugs as tubulin-polymerization inhibitors, focusing on the specific groups of 2-substituted benzimidazole based which are some related structural isomers of nocodazole analogues. The ADMET prediction shows that the toxicity for the structural isomers substituted at (2,7) or (2,4) positions (for **Ai** or **Di**) are significantly lower than at (2,6) or (2,5) positions (for **Bi** or **Ci**) for all substituents. The receptor-ligand interaction energies suggest that the representative compounds of **A10&D10**, **A8&D8**, and **A4&D4**, respectively, are the most reactive with significantly low toxicity compared to a true drug. These available drugs provide the lowest-energy conformations within colchicine-binding site that belongs to PDB code: 3E22, rather than PDB code: 5CA1, 1SA0, or 1SA1.

Keywords: Molecular docking; ADMET; tubulin-polymerization inhibitors; nocodazole analogues; benzimidazole

INTRODUCTION

Nocodazole is a well-known anticancer agent, and a member of 2-substituted benzimidazole derivatives (see Figure 1), named as methyl [5-(2-thienylcarbonyl)-1*H*-benzimidazol-2-yl] carbamate (Jordan *et al.*, 1992; Head *et al.*, 1985; Endo *et al.*, 2010). It is regarded as a specific antitubulin interfering with the structure and function of microtubules through inhibition of tubulin polymerization into normal microtubules. Nocodazole was bound directly to tubulin causing conformational changes resulting in increased exposure of some sulfhydryl (-SH) and possibly tyrosine (Tyr) residues (Margulis, 1973; Vasquez *et al.*, 1997). As a synthetic drug, nocodazole was confirmed as, for instance, the effective antitumoral drug interfering with microtubules on mammalian cells cultured *in vitro* (Brabanber *et al.*, 1976), the microtubule-active drug to increase p53 levels and play a major role in

Article history:

Received 19 September 2019; Received in revised from 28 May 2020;

Accepted 15 July 2020; Available online 15 July 2020

chemotherapeutic regimens (Tishler *et al.*, 1995), the reversible inhibitor of the colchicine binding site used for numerous *in vitro* studies (Mollinedo & Gajate, 2003), the effective anticancer drug enables to inhibit HeLa cells growth in a nanomolar range concentration for human cervical cancer (Lu *et al.*, 2018), etc.

For the specific group of benzimidazole derivatives in drug discovery, the factors that considerably play a vital role to exhibit a wide range of biological activities found in many natural and synthetic drugs are, for instance, (i) the prominent heterocyclic scaffold of benzimidazole based, (ii) the effect of 2-substituted benzimidazole scaffold that pharmacologically more potent rather than 1- or 3-substituted position, and (iii) the nitrogen-containing heterocycles that can easily interact with biomolecules of living system (Hadole *et al.*, 2018; Miao *et al.*, 2018; Hong, 2018; Kamal *et al.*, 2015; Srestha *et al.*, 2014). Moreover, benzimidazoles which contain a hydrogen atom attached to nitrogen in the 1-position readily tautomerize (see Figure 1), for example, 5-methylbenzimidazole is a tautomer of 6-methylbenzimidazole and thus both structures represent the same compound (Wright, 1951). Some representative equivalent tautomeric pairs in benzimidazole derivatives are listed in Table 1.

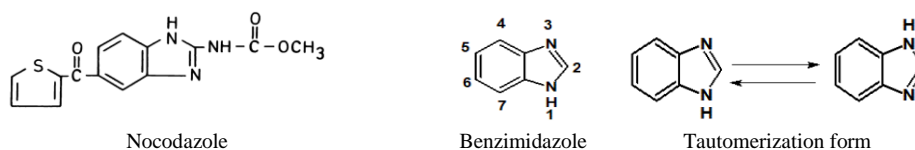


Figure 1 Structural formula of nocodazole (Brabanber *et al.*, 1976) and benzimidazole-based structure together with its tautomerization form (Wright, 1951; Hadole *et al.*, 2018)

In the present work, these predominant factors as well as the 1*H*-position readily tautomerize (N-containing heterocycle) of benzimidazole derivatives, are taken into account for modelling new related structural isomers of nocodazole analogues as tubulin-polymerization inhibitors (Nguyen *et al.*, 2005; Zefirova *et al.*, 2007; Botta *et al.*, 2008). Based on 2-substituted benzimidazole scaffold, a nocodazole (and its related compounds) can be spread into four structural isomers substituted at (2,4), (2,5), (2,6) and (2,7) positions, respectively, and two equivalent tautomeric pairs may be presumably regarded for isomers: (2,4) and (2,7), or (2,5) and (2,6). The molecular docking simulation will be performed for receptor-ligand interactions and incorporated with the ADMET prediction to evaluate druglike properties, *via* the Discovery Studio program (Wu *et al.* 2003; Sudprasert, 2011). For this *in silico* study, with respect to a nocodazole, it is expected to receive new lower toxic compounds and higher stability (stronger interaction) within colchicine-binding site of tubulin

heterodimers. In conclusion, the possibly reactive drugs are proposed as tubulin-polymerization inhibitors

Table 1 Some representative equivalent tautomeric pairs in benzimidazole derivatives

Position of substituent group(s) in first tautomer	Position of substituent group(s) in second tautomer	Designation
4	7	4 (or 7)
5	6	5 (or 6)
2,5	2,6	2,5 (or 2,6)
4,6	5,7	4,6 (or 5,7)
2,4,5	2,6,7	2,4,5 (or 2,6,7)
2,4,5,6	2,5,6,7	2,4,5,6 (or 2,5,6,7)

COMPUTATIONAL METHODS

Receptors and Ligands Modelling

Firstly, the four sets of α,β -tubulin heterodimers were prepared to be receptors, based on the X-ray diffraction structures of proteins, drugs and binding pockets taken from PDB code: 5CA1, 3E22, 1SA0 and 1SA1, respectively. The Discovery Studio Visualizer embedded in Discovery Studio (DS2018) program (copyrighted by Dassault Systèmes BIOVIA) was used for loading three-dimensional proteins, removing unwanted parts (such as, backbone, residues and drug-molecule), and then giving the α,β -tubulin heterodimers (Figure 2). Each available receptor consisted of two monomers (α - and β -units) of tubulin, and governed colchicine-binding site located at the α/β intradimer interface of tubulin heterodimers. In this study, the colchicine-binding site sphere was set of 14-Å radius as the active site for molecular docking simulation of receptor-ligand interactions.

Secondly, the 60 ligand models of related structural isomers of nocodazole analogues were created by BIOVIA Draw 2018 program (copyrighted by Dassault Systèmes BIOVIA), which can be divided into four templates: **A**, **B**, **C** and **D**, and designated by Ligand No. (1 - 60) or Ligand Index (**A1-A15**, **B1-B15**, **C1-C15** and **D1-D15**), as described in Table 2. The **A**, **B**, **C** and **D** templates were four structural isomers of nocodazole substituted at (2,7), (2,6), (2,5), and (2,4) positions, respectively, based on 2-substituted benzimidazole scaffold. Then, at 2-position for each template (or each structural isomer), there were fifteen representative groups of substituents: $-\text{NH}(\text{C}=\text{O})-\text{R}'$, as the same functional group based as in nocodazole, where R' was varied. The three-dimensional structures of new generated ligands were performed for the energy minimization *via* Ligand Minimization protocol, in DS2018 program.

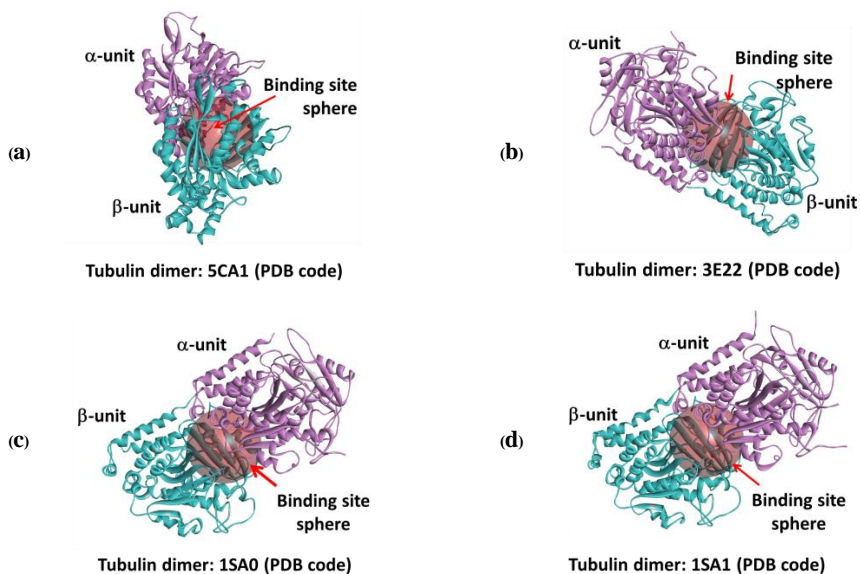
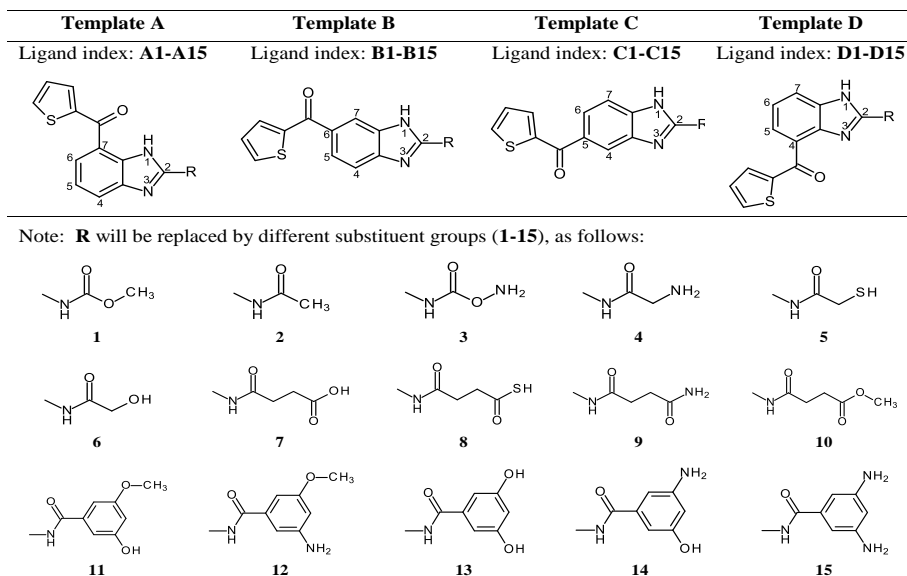


Figure 2 (a)-(d) The structures of α,β -tubulin heterodimers and binding site sphere (14-Å radius) for PDB code: 5CA1, 3E22, 1SA0, and 1SA1, respectively.

ADMET Prediction

The ADMET Descriptors protocol (in DS2018 program) uses the QSAR models to estimate a range of ADMET related properties for small molecules. The following properties, and classes of properties, can be computed: Aqueous solubility, Blood brain barrier penetration (BBB), Cytochrome P450 (CYP450) 2D6 inhibition, Hepatotoxicity, Human intestinal absorption (HIA), and Plasma protein binding (PPB). In this study, the ADMET Descriptors protocol is employed to evaluate the ADMET and physical properties of new generated isomers: **A1-A15**, **B1-B15**, **C1-C15** and **D1-D15**.

Table 2 The four structural isomers of nocodazole analogues with **A**, **B**, **C**, and **D** templates. Ligand index: **A1-A15**, **B1-B15**, **C1-C15**, and **D1-D15**.



Molecular Docking Method

The CDOCKER protocol with CHARMM forcefield (in DS2018 program) has been carried out for molecular docking method. CHARMM is a highly flexible molecular mechanics and dynamics program derived from the program CHARMM (Chemistry at HARvard Molecular Mechanics) and performs well over a broad range of calculations and simulations, including calculation of geometries, interaction and conformation energies, local minima, barriers to rotation, time-dependent dynamic behavior, and free energy [Wu *et al.*, 2003; Momany & Rone, 1992]. CHARMM is designed to give good results for a wide variety of modelled systems, from isolated small molecules to solvated complexes of large biological macromolecules.

The Dock Ligands (CDOCKER) uses a CHARMM-based molecular dynamics (MD) scheme to dock ligands into a receptor binding site. Random ligand conformations are generated using high-temperature MD. The conformations are then translated into the binding site. Candidate poses are then created using random rigid-body rotations followed by simulated annealing. A final minimization is then used to refine the ligand poses.

Table 3 The ADMET and physicochemical properties of all ligands, from this work. Ligand No. (Ligand Index): 1-15 (**A1-A15**), 16-30 (**B1-B15**), 31-45 (**C1-C15**), 46-60 (**D1-D15**).

Ligand No.	Ligand Index	MW.	Tox_P	CYP_P	PPB_P	BBB	Sol	Abs	AlogP	PSA
1	A1	301.3	7.3	-10.2	7.5	3	2	0	2.8	83
2	A2	285.3	5.4	-9.1	5.2	3	3	0	2.1	74
3	A3	302.3	5.7	-9.9	6.2	3	2	0	1.9	109
4	A4	300.3	3.7	-9.7	4.2	3	3	0	1.2	100
5	A5	317.4	4.0	-8.5	4.7	3	2	0	2.4	74
6	A6	301.3	4.0	-9.7	4.3	3	3	0	1.5	95
7	A7	343.4	2.3	-11.7	5.9	4	3	0	2.0	112
8	A8	359.4	4.5	-8.4	6.0	3	2	0	2.6	91
9	A9	342.4	4.6	-10.4	2.9	4	3	0	1.4	118
10	A10	357.4	2.5	-10.4	6.2	3	3	0	2.2	100
11	A11	393.4	5.6	-9.5	5.7	4	2	0	3.5	103
12	A12	392.4	5.5	-11.5	6.6	4	2	0	3.0	109
13	A13	379.4	5.5	-8.7	3.5	4	2	1	3.3	115
14	A14	378.4	5.9	-10.2	3.6	4	2	1	2.8	121
15	A15	377.4	7.1	-11.3	3.9	4	2	1	2.3	127
16	B1	301.3	14.0	-10.9	12.6	3	2	0	2.8	83
17	B2	285.3	10.3	-9.0	8.7	3	3	0	2.1	74
18	B3	302.3	11.5	-10.2	10.5	3	2	0	1.9	109
19	B4	300.3	8.6	-9.6	7.7	3	3	0	1.2	100
20	B5	317.4	9.0	-8.4	8.2	3	2	0	2.4	74
21	B6	301.3	9.0	-9.6	7.8	3	3	0	1.5	95
22	B7	343.4	7.3	-11.6	9.4	4	3	0	2.0	112
23	B8	359.4	9.4	-8.3	9.5	3	2	0	2.6	91
24	B9	342.4	9.6	-10.3	6.4	4	3	0	1.4	118
25	B10	357.4	7.4	-10.3	9.7	3	3	0	2.2	100
26	B11	393.4	10.6	-9.4	9.2	4	2	0	3.5	103
27	B12	392.4	10.5	-11.4	10.1	4	2	0	3.0	109
28	B13	379.4	10.4	-8.6	7.0	4	2	1	3.3	115
29	B14	378.4	10.9	-10.1	7.1	4	2	1	2.8	121
30	B15	377.4	12.1	-11.2	7.4	4	2	1	2.3	127
31	C1	301.3	14.0	-10.9	12.6	3	2	0	2.8	83
32	C2	285.3	10.3	-9.0	8.7	3	3	0	2.1	74
33	C3	302.3	11.5	-10.2	10.5	3	2	0	1.9	109
34	C4	300.3	8.6	-9.6	7.7	3	3	0	1.2	100
35	C5	317.4	9.0	-8.4	8.2	3	2	0	2.4	74
36	C6	301.3	9.0	-9.6	7.8	3	3	0	1.5	95
37	C7	343.4	7.3	-11.6	9.4	4	3	0	2.0	112
38	C8	359.4	9.4	-8.3	9.5	3	2	0	2.6	91
39	C9	342.4	9.6	-10.3	6.4	4	3	0	1.4	118
40	C10	357.4	7.4	-10.3	9.7	3	3	0	2.2	100
41	C11	393.4	10.6	-9.4	9.2	4	2	0	3.5	103
42	C12	392.4	10.5	-11.4	10.1	4	2	0	3.0	109
43	C13	379.4	10.4	-8.6	7.0	4	2	1	3.3	115
44	C14	378.4	10.9	-10.1	7.1	4	2	1	2.8	121
45	C15	377.4	12.1	-11.2	7.4	4	2	1	2.3	127
46	D1	301.3	7.3	-10.2	7.5	3	2	0	2.8	83
47	D2	285.3	5.4	-9.1	5.2	3	3	0	2.1	74
48	D3	302.3	5.7	-9.9	6.2	3	2	0	1.9	109
49	D4	300.3	3.7	-9.7	4.2	3	3	0	1.2	100
50	D5	317.4	4.0	-8.5	4.7	3	2	0	2.4	74
51	D6	301.3	4.0	-9.7	4.3	3	3	0	1.5	95
52	D7	343.4	2.3	-11.7	5.9	4	3	0	2.0	112
53	D8	359.4	4.5	-8.4	6.0	3	2	0	2.6	91
54	D9	342.4	4.6	-10.4	2.9	4	3	0	1.4	118
55	D10	357.4	2.5	-10.4	6.2	3	3	0	2.2	100
56	D11	393.4	5.6	-9.5	5.7	4	2	0	3.5	103
57	D12	392.4	5.5	-11.5	6.6	4	2	0	3.0	109
58	D13	379.4	5.5	-8.7	3.5	4	2	1	3.3	115
59	D14	378.4	5.9	-10.2	3.6	4	2	1	2.8	121
60	D15	377.4	7.1	-11.3	3.9	4	2	1	2.3	127

Note: **Tox_P** (Hepatotoxicity), **CYP_P** (CYP2D6 binding), **PPB_P** (Plasma protein binding), **BBB** (Blood-brain barrier level), **Sol** (Aqueous solubility level), **Abs** (Human intestinal absorption level), **AlogP** (AlogP98), **PSA** (Polar surface area)

Throughout this work, the molecular docking simulations have been performed to calculate the receptor-ligand interactions between α,β -tubulin heterodimers and ligand within four different sizes of binding pockets for PDB code: 5CA1, 3E22, 1SA0 and 1SA1. All atoms of proteins were held fixed as rigid body, while docked ligand was fully flexible. After simulation completed, the docked ligand poses (or the most stable conformations) with lowest receptor-ligand interaction energies have been collected. The calculated results have been interpreted in terms of the structural and energetic properties, including the formation of ligand-residues hydrogen bonding within the active sites.

RESULTS AND DISCUSSION

ADMET Prediction for Related Structural Isomers of Nocodazole Analogues

The ADMET prediction is used to evaluate the important physicochemical properties of new generated 60 ligands. ADMET properties are included of Absorption, Distribution, Metabolism, Excretion and Toxicity. The predicted values of ADMET and physicochemical properties of all 60 ligands, denoted by Ligand No. (or Ligand Index): 1-15 (**A1-A15**), 16-30 (**B1-B15**), 31-45 (**C1-C15**), 46-60 (**D1-D15**), are reported in Table 3. Herein, the isomers of four different templates will be denoted as **Ai**, **Bi**, **Ci**, and **Di**, where *i* means the substituent groups (*i* = 1, 2,..., 60), such as **A1**, **B1**, **C1**, and **D1**.

The Identical Properties for the Equivalent Tautomer Pairs

In Table 3, it is obviously found that all equivalent tautomer pairs; **Ai** and **Di**, or **Bi** and **Ci**, show totally identical values of ADMET and physicochemical properties. For instances, **A1** and **D1** isomers give the identical properties, i.e. Hepatotoxicity (Tox_P = 7.3), CYP2D6 binding (CYP_P = -10.2), Plasma protein binding (PPB_P = 7.5), Blood-brain barrier level (BBB = 3), Aqueous solubility level (Sol = 2), Human intestinal absorption Level (Abs = 0), AlogP98 (AlogP = 2.8), and Polar surface area (PSA = 8.3). Whereas **B1** and **C1** isomers give the identical properties, i.e. Tox_P = 14.0, CYP_P = -10.9, PPB_P = 12.6, BBB = 3, Sol = 2, Abs = 0, AlogP = 2.8, and PSA = 8.3.

Basically, the four structural isomers; **A1**, **B1**, **C1**, and **D1**, share the same molecular identities such as a number of atoms and molecular weight, as well as molecular formula, therefore, the predicted values of BBB, Sol, Abs, AlogP and PSA are actually identical.

Lowering the Toxicity for Ai (or Di) compared to Bi (or Ci)

Considering to the hepatotoxicity prediction (Tox_P) for all 60 ligands as reported in Table 3, it is obviously found that the predicted values of Tox_P for **Ai** (or **Di**) are approximately 1.7 to 2.3 times lower than **Bi** (or **Ci**), for any functional groups of substituents. It is suggested that the structural isomers substituted at (2,7) or (2,4) positions (for **Ai** or **Di**) tend to lower the toxicity, compared to the ones substituted at (2,6) or (2,5) positions (for **Bi** or **Ci**). For examples, the predicted values of Tox_P are

for **A1:B1** (7.3:14.0), **A2:B2** (5.4:10.3), **A3:B3** (5.7:11.5), **A4:B4** (3.7:8.6), **A5:B5** (4.0:9.0), **A6:B6** (4.0:9.0), **A7:B7** (2.3:7.3), **A8:B8** (4.5:9.4), **A9:B9** (4.6:9.6), **A10:B10** (2.5:7.4), **A11:B11** (5.6:10.6), **A12:B12** (5.5:10.5), **A13:B13** (5.5:10.4), **A14:B14** (5.9:10.9), and **A15:B15** (7.1:12.1).

Druglikeness Criteria for New Available Drugs

According to the predicted values of ADMET and physicochemical properties evaluated by ADMET Descriptor protocol, therefore, the druglike properties must be considered to identify the new available drugs. In this work, the criteria of druglikeness are summarized as in Table 4, corresponding to the values or levels of ADMET properties described in DS2018 program. It is found that, for all 60 ligands, only 10 ligands are satisfied with the druglikeness criteria, belonging to the members of **A** and **D** templates with substituent groups: **4**, **5**, **6**, **8**, and **10**. They are **A4**, **A5**, **A6**, **A8**, **A10**, **D4**, **D5**, **D6**, **D8**, and **D10**, respectively. The Tox_P values (between 2.5 and 4.5) of these available drugs are significantly lower than a drug; nocodazole (Tox_P = 14.0), causing less effect on dose-dependent liver injuries.

Table 4 The criteria of druglikeness considered in this work.

Value (or Level)	Description
Tox_P \leq 4.15	Unlikely to cause dose-dependent liver injuries
4.15 < Tox_P < 5.0	Slightly cause dose-dependent liver injuries
CYP_P \leq 0.16	Unlikely to inhibit CYP2D6 enzyme
PPB_P \leq -2.21	Bounded (< 90% bound) to plasma proteins
0 \leq BBB \leq 3	Inside 99% confidence ellipse
2 \leq Sol \leq 4	Acceptable aqueous solubility
0 \leq Abs \leq 2	Acceptable human intestinal absorption

The remarkable failure of other ligands is caused by; (i) the overflow of blood-brain barrier penetration level (BBB = 4) bringing them to be outside 99% confidence ellipse (or very low penetrant), or (ii) the hepatotoxicity beyond the consideration in this work (Tox_P \geq 5.0), likely to cause dose-dependent liver injuries.

Molecular Docking for Related Structural Isomers of Nocodazole Analogues

According to the chosen PDB codes: 5CA1, 3E22, 1SA0, and 1SA1, hence, the difference in size, shape, and amino acid residues exposed within the binding sites plays an important role for ligand binding affinity. As the rigid model of receptor, in this work, the variety of binding pockets is needed to compensate as for the flexible one. The interactions between α , β -tubulin heterodimers and individual ligand in colchicine-binding sites for PDB code: 5CA1, 3E22, 1SA0, and 1SA1, have been simulated. Overall results of the receptor-ligand interaction energy (in kcal/mol) for all ligands are illustrated in Figure 3.

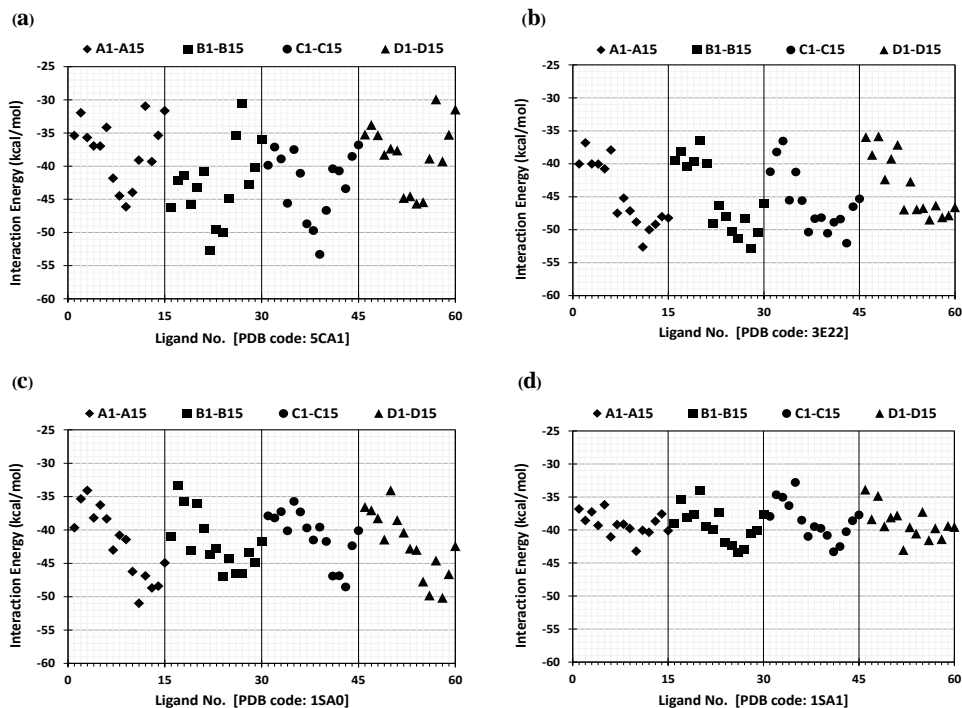


Figure 3 (a)-(d) Plots of the receptor-ligand interaction energies (in kcal/mol) for all 60 docked poses obtained from molecular docking simulation, for PDB code: 5CA1, 3E22, 1SA0, and 1SA1, respectively. Ligand No.: 1-15 (**A1-A15**); 16-30 (**B1-B15**); 31-45 (**C1-C15**); 46-60 (**D1-D15**).

Receptor-Ligand Interaction Energies for All Docked Ligands

Based on the similarity of functional groups of substituents, herein, it can be classified roughly into 3 groups:

Group I: 1, 2, 3, 4, 5, 6 (shared the same group; $-\text{NH}(\text{CO})-\text{R}'$)

Group II: 7, 8, 9, 10 (shared the same group; $-\text{NH}(\text{CO})\text{C}_2\text{H}_4(\text{CO})-\text{R}'$)

Group III: 11, 12, 13, 14, 15 (shared the same group; $-\text{NH}(\text{CO})\text{Ph}-\text{R}'\text{R}''$)

The results show that the receptor-ligand interaction energies of all docked ligands for PDB code: 5CA1, 3E22 and 1SA0 are highly distributed, except for PDB code: 1SA1, as shown in Figure 3 (a)-(d). In *Group I*, the docked ligands for **A**, **B**, **C**, and **D** templates usually provide high interaction energies (or less stability) for any PDB codes, except the **B1-B6** docked ligands for PDB code: 5CA1, which provide lowest-energy conformations. In *Group II*, the docked ligands for all templates always provide lower interaction energies (more stability) than those in *Group I*, for any PDB codes. Especially, for PDB code 5CA1, the docked ligands for **A**, **B**, **C**, and **D** templates in *Group II* provide the lowest-energy conformations, supporting to the high stability of these ligands within binding pocket of a real drug; nocodazole. In *Group III*, the docked ligands for all templates usually provide lower interaction energies

than *Group I*, for PDB code: 3E22, 1SA0, and 1SA1, whereas provide as high interaction energies as those in *Group I*, for PDB code: 5CA1.

Considering to the lowest-energy conformation, it is found that the most stable docked ligands (with interaction energy in kcal/mol) for each template are; for PDB code: 5CA1, i.e. **A9** (-46.1), **B7** (-52.7), **C9** (-53.3) and **D9** (-45.7); for PDB code: 3E22, i.e. **A11** (-52.6), **B13** (-52.8), **C13** (-52.0) and **D11** (-48.5); for PDB code: 1SA0, i.e. **A11** (-51.0), **B9** (-46.9), **C13** (-48.5) and **D13** (-50.2); and for PDB code: 1SA1, i.e. **A10** (-43.2), **B11** (-43.5), **C11** (-43.3) and **D7** (-43.0).

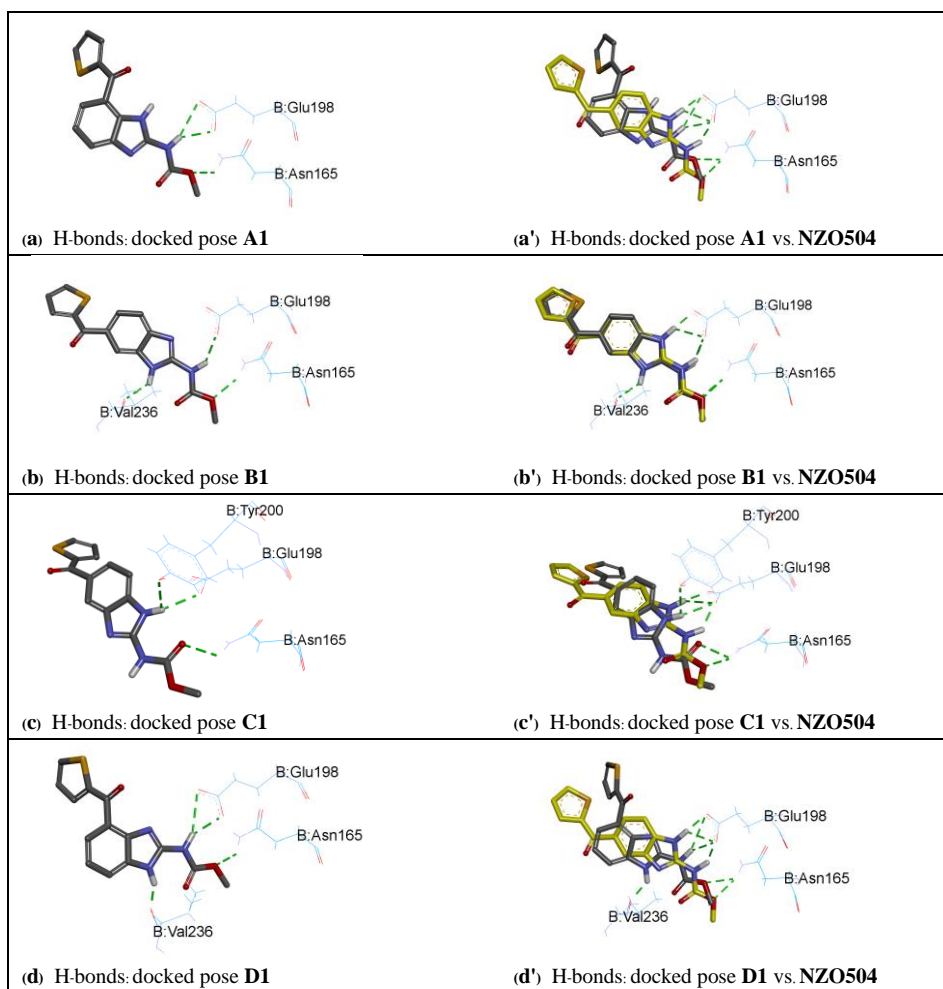


Figure 4 For PDB code: 5CA1. (a)-(d) Intermolecular hydrogen bonds of the docked poses of nocodazole isomers: **A1**, **B1**, **C1**, and **D1**, respectively. (a'- d') Superposition between the host-drug: **NZO504** (nocodazole; in yellowed carbons) and docked poses: **A1**, **B1**, **C1**, and **D1**, respectively, within colchicine-binding site of tubulin heterodimers.

Comparison of Hydrogen Bonding for Nocodazole Isomers with NZO504

The hydrogen bond formations of the docked poses of nocodazole isomers: **A1**, **B1**, **C1** and **D1**, with amino acid residues are illustrated in Figure 4, together with the superposition between these docked poses and a host-drug; nocodazole (NZO504), for PDB code: 5CA1. It is clearly seen that, for **A1**, **B1**, **C1** and **D1**, the hydrogen bonds are formed in β -tubulin region, in which ASN165 and GLU198 are formed with every isomers, while VAL236 formed H-bonds to both **B1** and **D1**, and TYR200 only formed H-bond to **C1**. It is confirmed in this work that the residues; ASN165(β) and GLU198(β), always formed H-bonds to nocodazole (and its isomers) corresponding with the X-ray diffraction structure of active drug NZO504. Moreover, the superposition between the docked poses and NZO504 suggests that the best fit of ligand conformation belongs to **B1**. The calculated overlay similarities for the docked poses of **A1**, **B1**, **C1** and **D1**, with respect to NZO504 (PDB code: 5CA1), are 0.60, 0.85, 0.74 and 0.66, respectively. The order of stability are **B1** > **C1** > **A1** > **D1**, with interaction energies of -46.2, -39.9, -35.4, and -35.2 kcal/mol, respectively.

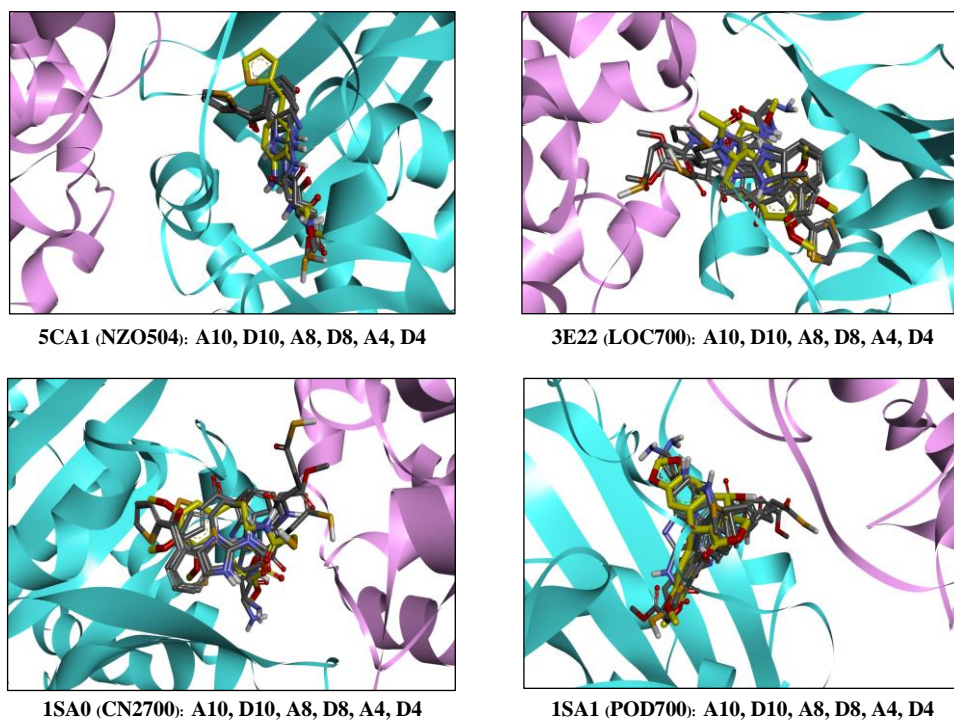


Figure 5 Superposition of the docked poses; **A10**, **D10**, **A8**, **D8**, **A4**, and **D4**, with the host-drugs (in yellowed carbons); NZO504 (nocodazole), LOC700 (colchicine), CN2700 (DAMA-colchicine), and POD700 (podophyllotoxin) for PDB code: 5CA1, 3E22, 1SA0 and 1SA1, respectively, within colchicine-binding site of tubulin heterodimers.

Receptor-Ligand Interactions and H-bonds for New Available Drugs

As discussed earlier, the 10 ligands that satisfied with the druglikeness criteria are **A4**, **A5**, **A6**, **A8**, **A10**, **D4**, **D5**, **D6**, **D8** and **D10**, respectively. Considering to the receptor-ligand interaction energies for these docked ligands, it is found that only 3 equivalent tautomeric pairs (or 6 docked ligands) provide significantly stronger interactions (lowest-energy conformations) within four binding sites (PDB code: 5CA1, 3E22, 1SA0, and 1SA1), compared to tautomer pair of nocodazole; **A1&D1**. The order of stability are; **A10&D10** > **A8&D8** > **A4&D4**.

Figure 5 illustrates the orientations of the docked poses; **A10**, **D10**, **A8**, **D8**, **A4**, and **D4**, overlaid with the host-drugs within colchicine-binding sites for PDB code: 5CA1 (nocodazole; NZO504), 3E22 (colchicine; LOC700), 1SA0 (DAMA-colchicine; CN2700), and 1SA1 (podophyllotoxin; POD700), respectively. For PDB code: 5CA1 and 1SA1, all available drugs are trapped within β -tubulin region, while for PDB code: 3E22 and 1SA0, some molecules may shift toward α -tubulin region. Details of the receptor-ligand interaction energies (E_{int}) and hydrogen-bonded residues for the docked poses of **A10**, **D10**, **A8**, **D8**, **A4**, and **D4**, are reported in Table 5, together with the host-drugs.

Table 5 Summary of the receptor-ligand interaction energies (E_{int}) for the docked poses of **A10**, **D10**, **A8**, **D8**, **A4** and **D4**, and hydrogen-bonded residues, together with host-drugs: Nocodazole, Colchicine, DAMA-colchicine, or Podophyllotoxin, for PDB code: 5CA1, 3E22, 1SA0 and 1SA1, respectively.

Ligand No.	Ligand Index	5CA1		3E22		1SA0		1SA1	
		E_{int}	H-bond	E_{int}	H-bond	E_{int}	H-bond	E_{int}	H-bond
10	A10	-44.0	B:ASN165[2]; TYR200; VAL236	-48.8	B:LYS254; A:ASN101	-43.2	A:ASN101	-46.2	B:ALA316 (weak); THR376 (weak)
55	D10	-45.4	B:ASN165[2]; GLU198; TYR200; VAL236	-46.7	B:LYS254; A:ASN101	-37.3	A:VAL181	-47.7	B:THR353
8	A8	-44.5	B:ASN165[2]; GLU198[2]; TYR200	-45.2	B:ASN249; LYS254; A:GLN11; ASN101; THR179	-39.1	B:ASN249; LYS254[2]; A:GLN11	-40.8	B:THR353; A:THR179
53	D8	-44.6	B:GLN134; ASN165[2]; GLU198[2]; TYR200; VAL236	-42.7	B:LYS254 (weak)	-39.6	A:ASN101; SER178; THR179	-42.8	no H-bond
4	A4	-37.0	B:ASN165; GLU198[2]; TYR200	-40.0	B:ASN258; VAL315[3]; ASN350	-39.3	B:ALA250 (weak); VAL315 (weak)	-38.2	B:ASN258[2]; LYS352
49	D4	-38.3	B:ASN165; GLU198[2]; TYR200; VAL236	-42.4	B:ASN258[2]; MET259	-39.4	B:LEU255; VAL315; ASN350; LYS352	-41.4	B:ASN258[2]; ASN349; LYS352
Nocodazole		B:ASN165; GLU198[3]							
Colchicine				B:ASN258					
DAMA-colchicine						A:VAL181			
Podophyllotoxin								B:CYS241	

Note: For examples, B:ASN165[2] means the amino acid residue ASN165(β) formed two H-bonds to a drug. A:ASN101 means the residue ASN101(α) formed one H-bond to a drug. B:ALA250(weak) means the residue ALA250(β) formed a weak H-bond to a drug.

From overall calculated results, it could be mentioned that the 3 equivalent tautomeric pairs; **A10&D10**, **A8&D8**, and **A4&D4**, provide the lowest-energy conformations within colchicine-binding site that belongs to PDB code: 3E22, as illustrated in Figure 6. The lowest interaction energies are -48.8, -45.2, and -42.4 kcal/mol, for the representative conformations of **A10&D10**, **A8&D8**, and **A4&D4**, respectively.

It is found that for **A10&D10** isomers, LYS254(β) and ASN101(α) provide the most probability to form H-bonds with O atoms (from $-\text{OCH}_3$ and $-\text{C}=\text{O}$) of substituents. For **A8&D8** isomers, LYS254(β) provides the most probability to form H-bond with O atom ($-\text{C}=\text{O}$) of substituent for both isomers, while the H-bonds are formed between THR179(α) \cdots HN-, ASN249(β) \cdots S(H)-, ASN101(α) \cdots O=C-, and GLN11(α) \cdots HS-, respectively, along a side chain for **A8** isomer. For **A4&D4** isomers, ASN258(β) provides the most probability to form H-bond with O and/or H atoms (from $-\text{C}=\text{O}$ and $-\text{NH}_2$) of substituent, while VAL315(β) and ASN350(β) form two H-bonds with N and H atoms (from $-\text{NH}_2$) of a side chain for **A4** isomer, but only MET259(β) forms H-bond with H atom of $-\text{NH}_2$ group for **D4** isomer.

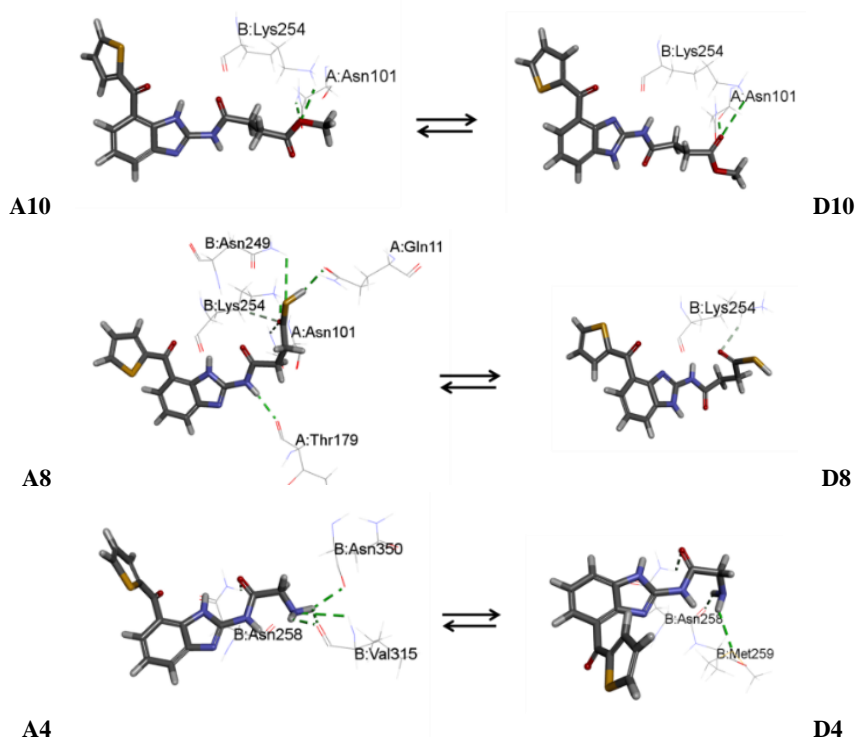


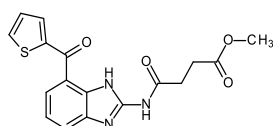
Figure 6 The lowest-energy conformations of the 3 equivalent tautomeric pairs; **A10&D10**, **A8&D8**, and **A4&D4**, and H-bond formation within binding sites, for PDB code: 3E22.

The New Available Drugs as Tubulin-Polymerization Inhibitors

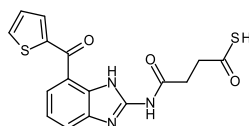
According to the ADMET prediction and molecular docking simulation, therefore, the new available drugs as tubulin-polymerization inhibitors are predicted in terms of the equivalent tautomeric pairs. With significantly low toxicity, the most reactive compounds are **A10&D10**, and the less reactive compounds are **A8&D8** and **A4&D4**, respectively. The ADMET properties and structural formula of new available drugs as tubulin-polymerization inhibitors are summarized in Table 6, together with a drug; nocodazole.

Table 6 Summary of the ADMET properties and structural formula of new available drugs as tubulin-polymerization inhibitors, together with a drug; nocodazole.

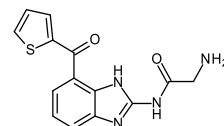
Ligand No.	Ligand Index	No. atoms	Mol. Formula	MW	ADMET Properties								
					Tox_P	CYP_P	PPB_P	BBB	Sol	Abs	AlogP	PSA	
10	A10	40	C17 H15 N3 O4 S	357.4	2.5	-10.4	6.2	3	3	0	2.2	100	
55	D10	40	C17 H15 N3 O4 S	357.4	2.5	-10.4	6.2	3	3	0	2.2	100	
8	A8	37	C16 H13 N3 O3 S2	359.4	4.5	-8.4	6.0	3	2	0	2.6	91	
53	D8	37	C16 H13 N3 O3 S2	359.4	4.5	-8.4	6.0	3	2	0	2.6	91	
4	A4	33	C14 H12 N4 O2 S	300.3	3.7	-9.7	4.2	3	3	0	1.2	100	
49	D4	33	C14 H12 N4 O2 S	300.3	3.7	-9.7	4.2	3	3	0	1.2	100	
	Nocodazole	32	C14 H11 N3 O3 S	301.3	14.0	-10.9	12.6	3	2	0	2.8	83	



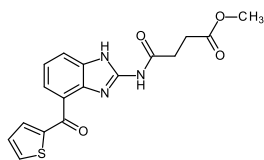
A10 (Tox_P = 2.5)



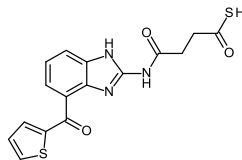
A8 (Tox_P = 4.5)



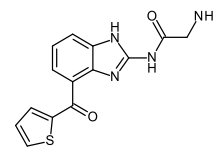
A4 (Tox_P = 3.7)



D10 (Tox_P = 2.5)



D8 (Tox_P = 4.5)



D4 (Tox_P = 3.7)

CONCLUSIONS

As for the *in silico* drug design, the molecular docking study and ADMET prediction have been successfully collaborated in order to investigate the acceptable low toxic drugs and the lowest-energy conformations. The ADMET prediction shows that the toxicity for **Ai** (or **Di**) are approximately 1.7 to 2.3 times lower than **Bi** (or **Ci**) for all substituents, which suggests that the structural isomers substituted at (2,7) or (2,4) positions (for **Ai** or **Di**) tend to lower the toxicity, compared to the ones substituted at (2,6) or (2,5) positions (for **Bi** or **Ci**). As tubulin-polymerization inhibitors, the representative compounds of **A10&D10**, **A8&D8**, and **A4&D4**, respectively, are the most reactive with significantly low toxicity comparing with a

drug; nocodazole. These equivalent tautomer pairs provide the lowest-energy conformations within colchicine-binding site that belongs to PDB code: 3E22.

ACKNOWLEDGMENTS

This work was financially supported by the Research Grant of Burapha University through National Research Council of Thailand (Grant no. 188/2561). Computational results obtained using software programs from Dassault Systèmes BIOVIA.

REFERENCES

- Botta, M., Forli, S., Magnani, M. & Manetti, F. (2008). Molecular Modeling Approaches to Study the Binding Mode on Tubulin of Microtubule Destabilizing and Stabilizing Agents. Springer-Verlag Berlin Heidelberg, New York.
- Brabanber, M.J.D., Van de Veire, R.M.L., Aerts, F.E.M., Borgers, M. & Janssen, P.A.J., (1976). The Effects of Methyl (5-(2-Thienylcarbonyl)-1H-benzimidazol-2-yl] carbamate, (R17934; NSC238159), a New Synthetic Antitumoral Drug Interfering with Microtubules, on Mammalian Cells Cultured *in Vitro*. *Cancer Research*. **36**, 905-916.
- Endo, K., Mizuguchi, M., Harata, A., Itoh, G. & Tanaka, K. (2010). Nocodazole induces mitotic cell death with apoptotic-like features in *Saccharomyces cerevisiae*. *Federation of European Biochemical Societies Letters*. **584**, 2387-2392.
- Hadole, C.D., Rajput, J.D. & Bendre, R.S. (2018). Concise on Some Biologically Important 2-Substituted Benzimidazole Derivatives. *Organic Chemistry: Current Research*. **7:3**.
- Head, J., Lee, L.L.Y., Field, D.J. & Lee, J.C. (1985). Equilibrium and Rapid Kinetics Studies on Nocodazole-Tubulin Interaction. *Journal of Biological Chemistry*. **260**, 11060-11066.
- Hong, S.T. (2018). Albendazole & Praziquantel: Review and Safety Monitoring in Korea. *Infection Chemotherapy*. **50**, 1-10.
- Jordan, M.J., Thrower, D. & Wilson, L. (1992). Effects of vinblastine, podophyllotoxin and nocodazole on mitotic spindles. *Journal of Cell Science*. **102**, 401-416.
- Kamal, A., Reddy, T. S., Vishnuvardhan, M.V.P.S., Nimbarte, V. D., Rao, A.V.S., Srinivasulu, V. & Shankaraiah, N. (2015). Synthesis of 2-aryl-1,2,4-oxadiazolo-benzimidazoles: Tubulin polymerization inhibitors and apoptosis inducing agents. *Bioorganic & Medicinal Chemistry*. **23**, 4608-4623.
- Lu, J., Torre, J.D.L., Mc Cann, C., Madar, M. & Zhou, Q. (2018). A Quantitative Study of Nocodazole's Effect on HeLa Cells' Growth Rate and F-actin Structure. *American Journal of Life Sciences*. **6**, 7-12.
- Margulis, L., (1973). Colchicine-sensitive Microtubules. *International Review of Cytology* **34**, 333-361.

- Miao, T.T., Tao, X.B., Li, D.D., Chen, H., Jin, X.Y., Geng, Y., Wang, S.F. & Gu, W. (2018). Synthesis and biological evaluation of 2-arylbenzimidazole derivatives of dehydroabiatic acid as novel tubulin polymerization inhibitors. *Royal Society of Chemistry Advanced*. **8**, 17511-17526.
- Mollinedo, F. & Gajate, C. (2003). Microtubules, microtubule-interfering agents and apoptosis. *Apoptosis*. **8**, 413-450.
- Momany, F.A., & Rone, R.J. (1992). Validation of the general-purpose QUANTA 3.2/ CHARMM force field. *Computational Chemistry*. **13**, 888-900.
- Nguyen, T.L., McGrath, C., Hermone, A.R., Burnett, J.C., Zaharevitz, D.W., Day, B.W., Wipf, P., Hamel, E. & Gussio, R. (2005). A common pharmacophore for a diverse set of colchicine site inhibitors using a structure-based approach, *Journal of Medicinal Chemistry*. **50**, 6107-6116.
- Srestha, N., Banerjee, J. & Srivastava, S. (2014). A review on chemistry and biological significance of benzimidazole nucleus. *IOSR Journal of Pharmacy*. **4**, 28-41.
- Sudprasert, P. (2011). Design of Microtubule Inhibitors as anticancer Drugs. Thesis M.Sc. (Chemistry), Faculty of Science, Burapha University, Chonburi, Thailand.
- Tishler, R.B., Lampp, D.M., Park, S. & Price, B.D. (1995). Microtubule-active Drugs Taxol, Vinblastine, and Nocodazole Increase the Levels of Transcriptionally Active p53. *Cancer Research*. **55**, 6021-6025.
- Vasquez, R.J., Howell, B., Yvon, A.-M. C., Wadsworth, P. & Cassimeris, L. (1997). Nanomolar Concentrations of Nocodazole Alter Microtubule Dynamic Instability *in Vivo* and *in Vitro*. *Molecular Biology of the Cell*. **8**, 973-985.
- Wright, J.B. (1951). The Chemistry of the Benzimidazoles. *Chemical Reviews*. **48**, 397-541.
- Wu, G., Robertson, D.H., Brooks, C.L. III & Vieth, M. (2003). Detailed Analysis of Grid-Based Molecular Docking: A Case Study of CDOCKER-A CHARMM-Based MD Docking Algorithm. *Journal of Computational Chemistry*. **24**, 1549-1562.
- Zefirova, O.N., Diikov, A.G., Zyk, N.V. & Zefirov, N.S. (2007). Ligands of the colchicine site of tubulin: a common pharmacophore and new structural classes, *Russian Chemical Bulletin, International Edition*. **56**, 680-688.